

## Recent STAR results and future prospects of $W^\pm$ boson production in polarized proton-proton collisions at RHIC

---

**Bernd Surrow (for the STAR Collaboration)\***

*Massachusetts Institute of Technology, 77 Massachusetts Avenue, Cambridge, MA 02139, USA*

*E-mail: [surrow@mit.edu](mailto:surrow@mit.edu)*

The STAR experiment at the Relativistic Heavy-Ion Collider at Brookhaven National Laboratory is providing fundamental measurements in high-energy polarized  $\vec{p} + \vec{p}$  collisions at  $\sqrt{s} = 200 - 500 \text{ GeV}$  to deepen our understanding on the spin structure and dynamics of the proton. This program has completed the first data taking period in 2009 of polarized  $\vec{p} + \vec{p}$  collisions at  $\sqrt{s} = 500 \text{ GeV}$ . This opens a new era in the study of the spin-flavor structure of the proton based on the production of  $W^{-(+)}$  bosons. The measurement of the cross section and single-spin asymmetries for midrapidity decay positrons and electrons from  $W^+$  and  $W^-$  boson production in longitudinally polarized  $\vec{p} + p$  collisions at  $\sqrt{s} = 500 \text{ GeV}$  is presented.

*35th International Conference on High Energy Physics, ICHEP 2010, July 22-28, 2010, Paris, France*

---

\*Speaker.

## 1. Introduction

Understanding the spin structure of the nucleon remains a fundamental challenge in Quantum Chromodynamics (QCD). Experimentally, polarized deep-inelastic scattering (pDIS) studies have shown that the quark spins account for only  $\approx 33\%$  of the proton spin [1]. Semi-inclusive pDIS measurements [2, 3, 4, 5] are sensitive to the quark and antiquark spin contributions separated by flavor [6, 7]. They rely on a quantitative understanding of the fragmentation of quarks and antiquarks into observable final-state hadrons. While the sum of the contributions from quark and antiquark parton distribution functions (PDFs) of the same flavor is well constrained, the uncertainties in the polarized antiquark PDFs separated by flavor remain relatively large [6, 7].

High energy polarized  $\vec{p} + \vec{p}$  collisions at  $\sqrt{s} = 200 - 500$  GeV at RHIC provide a unique way to probe the proton spin structure and dynamics using hard scattering processes [8]. The production of jets and hadrons is currently the prime focus of the gluon polarization studies. The production of  $W^{-(+)}$  bosons at  $\sqrt{s} = 500$  GeV provides an ideal tool to study the spin-flavor structure of the proton. This has been pointed out at the very early design stages of the polarized proton collider program at RHIC [9].

The data taking period in 2009 of polarized  $\vec{p} + \vec{p}$  collisions at  $\sqrt{s} = 500$  GeV opens a new era in the study of the spin-flavor structure of the proton based on the production of  $W^{-(+)}$  bosons.  $W^{-(+)}$  bosons are produced predominantly through  $\bar{u} + d$  ( $u + \bar{d}$ ) collisions and can be detected through their leptonic decay [10]. Quark and antiquark polarized PDFs are probed in calculable leptonic  $W$  decays at large scales set by the mass of the  $W$  boson. The production of  $W$  bosons in polarized proton collisions allows for the observation of purely weak interactions, giving rise to large, parity-violating, longitudinal single-spin asymmetries. A theoretical framework has been developed to describe inclusive lepton production,  $\vec{p} + p \rightarrow W^\pm + X \rightarrow l^\pm + X$ , that can be directly compared with experimental measurements using constraints on the transverse energy and pseudorapidity of the final-state leptons [11, 12]. This development profits from a rich history of hadroproduction of weak bosons at the CERN SPS and the FNAL Tevatron and provides a firm basis to use  $W$  production as a new high-energy probe in polarized  $\vec{p} + \vec{p}$  collisions [13].

## 2. Measurement of midrapidity decay $e^\pm$ from $W^\pm$ boson production

The data used for the first  $W$  boson production analysis at STAR were collected in 2009 colliding polarized proton beams at 250 GeV. The polarization of each beam was measured using Coulomb-Nuclear Interference proton-carbon polarimeters [14], which were calibrated using a polarized hydrogen gas-jet target [15]. Longitudinal polarization of proton beams in the STAR interaction region (IR) was achieved by spin rotator magnets upstream and downstream of the IR that changed the proton spin orientation from its stable vertical direction to longitudinal. Non-longitudinal beam polarization components were continuously monitored with a local polarimeter system at STAR based on the Zero-Degree Calorimeters with an upper limit on the relative contribution of 15% for both polarized proton beams [16, 17]. The longitudinal beam polarizations averaged over all runs were  $P_1 = 0.38$  and  $P_2 = 0.40$  with correlated relative uncertainties of 8.3% and 12.1%, respectively. Their sum  $P_1 + P_2 = 0.78$  is used in the analysis and has a relative uncertainty of 9.2%.

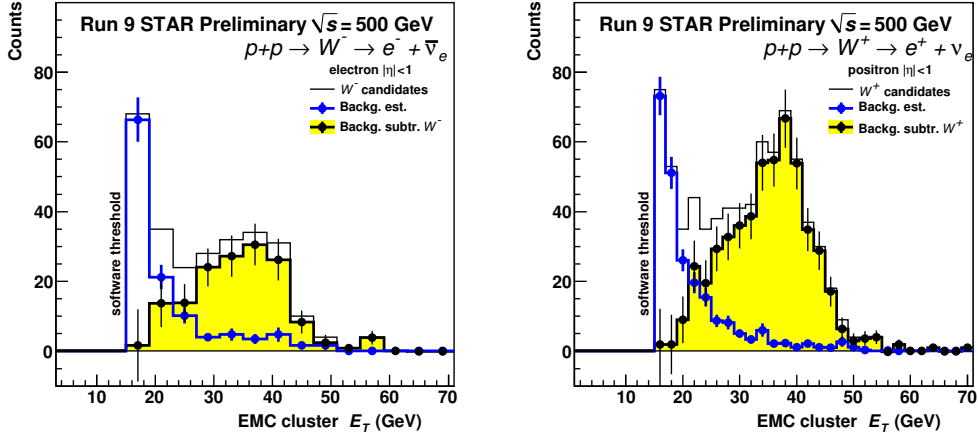


**Figure 1:** EMC cluster transverse energy distributions for  $W^-$  (left) and  $W^+$  (right) events showing the candidate histograms in black, the full background estimates in blue and the signal distributions in yellow.

Positrons ( $e^+$ ) and electrons ( $e^-$ ) from  $W^+$  and  $W^-$  boson production with  $|\eta_e| < 1$  are selected for this analysis. High- $p_T$   $e^\pm$  are charge-separated using the STAR TPC. The BEMC is used to measure the transverse energy  $E_T^e$  of  $e^+$  and  $e^-$ . The suppression of the QCD background is achieved with the TPC, BEMC, and EEMC.

The selection of  $W$  candidate events is based on kinematic and topological differences between leptonic  $W^\pm$  decays and QCD background events. Events from  $W^\pm$  decays contain a nearly isolated  $e^\pm$  with a neutrino in the opposite direction in azimuth. The neutrino escapes detection leading to a large missing energy. Such events exhibit a large imbalance in the vector  $p_T$  sum of all reconstructed final-state objects. In contrast, QCD events, e.g. di-jet events, are characterized by a small magnitude of this vector sum imbalance.

Candidate  $W$  events were selected online by a two-step energy requirement in the BEMC. Electrons or positrons from  $W$  production at midrapidity are characterized by large  $E_T$  peaked at  $\approx M_W/2$  (Jacobian peak). At the hardware trigger level, a high tower calorimetric trigger condition required  $E_T > 7.3$  GeV in a single BEMC tower. At the software trigger level, a dedicated trigger algorithm searched for a seed tower of  $E_T > 5$  GeV and computed all four possible combinations of  $2 \times 2$  tower cluster  $E_T$  sums above 13 GeV. A total of  $1.4 \times 10^6$  events were recorded for a data sample of approximately  $12 \text{ pb}^{-1}$ . A Vernier scan was used to determine the absolute luminosity with an accuracy for this preliminary result of currently 23% [18].

An electron candidate is defined to be any TPC track with  $p_T > 10 \text{ GeV}/c$  that is associated with a primary vertex with  $|z| < 100 \text{ cm}$ , where  $z$  is the distance along the beam direction. A  $2 \times 2$  BEMC tower cluster  $E_T$  sum,  $E_T^e$ , is required to be larger than 15 GeV, referred to as software threshold. The excess BEMC  $E_T$  sum in a  $4 \times 4$  tower cluster centered around the respective  $2 \times 2$  tower cluster is required to be below 5%. In addition, the distance between the  $2 \times 2$  cluster tower centroid and the TPC track is required to be less than 7 cm. A near-cone is formed around the electron candidate direction with a radius in  $\eta$ - $\phi$  space of  $R = 0.7$ . The excess BEMC, EEMC and TPC  $E_T$  sum in this cone is required to be less than 12% of the  $2 \times 2$  cluster  $E_T$ . The away-side  $E_T$  is the EMC plus TPC  $E_T$  sum over the full  $\eta$  range and  $\phi \in [\phi_e + \phi + 0.7, \phi_e + \pi - 0.7]$ . The vector  $p_T$  sum is defined as the sum of the  $e^\pm$  candidate  $p_T$  vector and the  $p_T$  vectors of

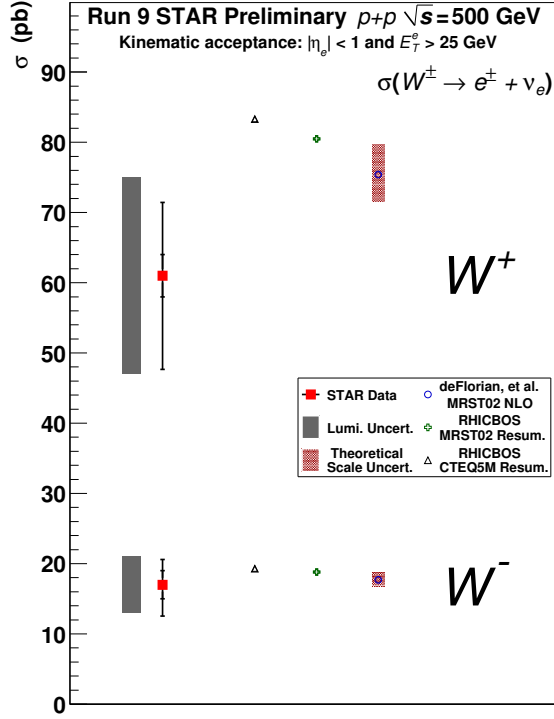


**Figure 2:** Measured cross sections for  $W^\pm$  production in comparison to predictions based on full resummed (RHICBOS) [11] and NLO (CHE) [20] predictions.

all the reconstructed jets with the thrust axes outside the  $R = 0.7$  cone around the candidate  $e^\pm$ . Jets were reconstructed using the standard mid-point cone algorithm used in previous STAR jet measurements. The final  $W$  candidate events are selected by requiring the away-side  $E_T$  to be less than 30 GeV and the magnitude of the vector  $p_T$  sum to be larger than 15 GeV.

Figure 1 presents the charge-separated lepton  $E_T^e$  distributions based on the selection criteria given above.  $W$  candidate events are shown as the black histograms, where the characteristic Jacobian peak can be seen at  $\approx M_W/2$ .

The number of background events was estimated through a combination of a PYTHIA 6.205 [19] MC simulation and a data-driven procedure. The  $e^{+(-)}$  background from  $W^{+(-)}$  boson induced  $\tau^{+(-)}$  decays was estimated using a MC simulations. The remaining background is mostly due to QCD dijet events where one of the jets missed the STAR acceptance. We have developed a data-driven procedure to evaluate this type of background. We excluded the EEMC ( $1 < \eta < 2$ ) as an active detector in our analysis to estimate the background due to missing calorimeter coverage for  $-2 < \eta < -1$ . The background contribution due to missing calorimeter coverage along with  $\tau$  background contributions have been subtracted from both  $W^{+(-)}$   $E_T^e$  distributions. The remaining background, presumably due to missing jets outside the STAR  $|\eta| < 2$  window, is evaluated based on an extrapolation from the region of  $E_T^e < 19$  GeV in both  $W^{+(-)}$   $E_T^e$  distributions. The shape is determined from the  $E_T^e$  distribution in events previously rejected as background. This shape  $E_T^e$  distribution is normalized to both  $W^{+(-)}$   $E_T^e$  distributions for  $E_T^e < 19$  GeV. The total background estimate for  $e^{+(-)}$  is shown in Fig. 1 by the blue line.

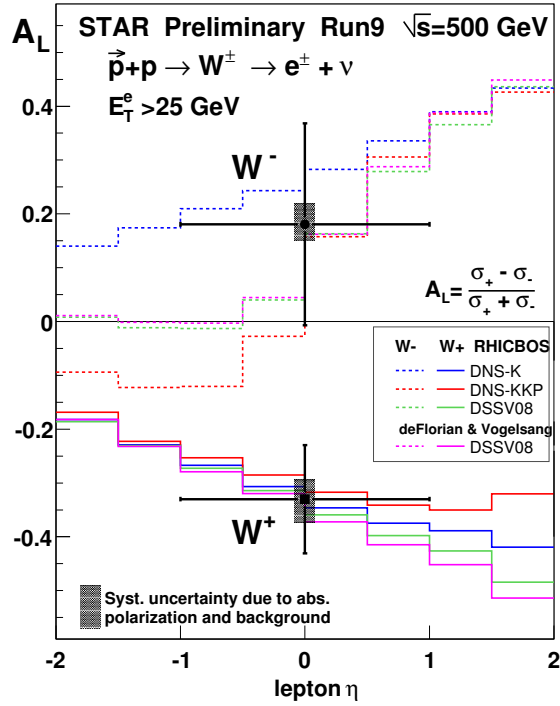


**Figure 3:** Longitudinal single-spin asymmetry,  $A_L$ , for  $W^\pm$  events as a function of the leptonic pseudorapidity,  $\eta_e$ , for  $25 < E_T^e < 50$  GeV in comparison to theory predictions (See text for details).

### 3. Midrapidity $W^\pm$ cross section and asymmetry measurements

Preliminary results for the production cross section of  $W^\pm \rightarrow e^\pm + X$  from candidate events with  $|\eta_e| < 1$  and  $E_T^e > 25$  GeV are shown in Fig. 2. The measured values are  $\sigma^{W^+} = 61 \pm 3$  (stat.)  $^{+10}_{-13}$  (syst.)  $\pm 14$  (lumi.) pb and  $\sigma^{W^-} = 17 \pm 2$  (stat.)  $^{+3}_{-4}$  (syst.)  $\pm 4$  (lumi.) pb. The statistical and systematic uncertainties are shown as the error bars on the red data points. The systematic uncertainty of the measured luminosity, shown separately as the grey bands in Fig. 2, is dominated by the uncertainty in the vernier scan measurement mentioned previously. The measured cross sections are consistent with predictions based on full resummed (RHICBOS) [11] and NLO (deFlorian & Vogelsang) [20] evaluations, which are also shown in Fig. 2. Theoretical scale uncertainties are shown for the NLO predictions as red shaded bands.

In Figure 3, the measured asymmetries are compared to predictions based on full resummed (RHICBOS) [11] and NLO (deFlorian & Vogelsang) [12] calculations. The NLO calculations use the DSSV08 polarized PDFs [5], whereas the resummed calculations are shown in addition for the older DNS-K and DNS-KKP [20] PDFs. The NLO and resummed results are in good agreement. The range spanned by the DNS-K and DNS-KKP distributions for  $\Delta\bar{d}$  and  $\Delta\bar{u}$  coincides, approximately, with the corresponding DSSV08 uncertainty estimates [6, 7]. The spread of predictions for  $A_L^{W^{+(-)}}$  is largest at forward (backward)  $\eta_e$  and is strongly correlated to the one found for the  $\bar{d}$  ( $\bar{u}$ ) polarized PDFs in the RHIC kinematic region in contrast to the backward (forward)  $\eta_e$  region dominated by the behavior of the well-known valence  $u$  ( $d$ ) polarized PDFs [12]. At midrapidity,  $W^{+(-)}$  production probes a combination of the polarization of the  $u$  and  $\bar{d}$  ( $d$  and  $\bar{u}$ ) quarks, and  $A_L^{W^{+(-)}}$  is

expected to be negative (positive) [6, 7]. The measured  $A_L^{W^+}$  is indeed negative stressing the direct connection to the  $u$  quark polarization. The central value of  $A_L^{W^-}$  is positive as expected with a larger statistical uncertainty. Our  $A_L$  results are consistent with predictions using polarized quark and antiquark PDFs constrained by inclusive and semi-inclusive pDIS measurements, as expected from the universality of polarized PDFs.

#### 4. Summary

In summary, we report the first measurement of midrapidity,  $|\eta_e| < 1$ , decay positrons and electrons from  $W^+$  and  $W^-$  boson production in longitudinally polarized  $\vec{p}+p$  collisions at  $\sqrt{s} = 500$  GeV by the STAR experiment at RHIC. This measurement establishes a new and direct way to explore the spin structure of the proton using parity-violating weak interactions in polarized  $\vec{p}+p$  collisions. The measured asymmetries agree well with NLO and resummed calculations using the DSSV08 polarized PDFs, which are probed at RHIC at much larger scales than in previous and ongoing pDIS experiments. Future high-statistics measurements at midrapidity together with measurements at forward and backward pseudorapidities will focus on constraining the polarization of  $\vec{d}$  and  $\vec{u}$  quarks.

#### References

- [1] Bass S D 2009 *Mod. Phys. Lett.* **A24** 1087
- [2] Adeva B *et al.* (Spin Muon Collaboration) 1998 *Phys. Lett.* **B420** 180–190
- [3] Airapetian A *et al.* (HERMES) 2005 *Phys. Rev.* **D71** 012003
- [4] Alekseev M G (COMPASS) 2010 *Phys. Lett.* **B693** 227–235
- [5] Alekseev M *et al.* (COMPASS) 2008 *Phys. Lett.* **B660** 458
- [6] de Florian D, Sassot R, Stratmann M and Vogelsang W 2008 *Phys. Rev. Lett.* **101** 072001
- [7] de Florian D, Sassot R, Stratmann M and Vogelsang W 2009 *Phys. Rev.* **D80** 034030
- [8] Bunce G *et al.* 2000 *Ann. Rev. Nucl. Part. Sci.* **50** 525
- [9] Underwood D *et al.* 1992 *Part. World.* **3** 1–12
- [10] Bourrely C and Soffer J 1993 *Phys. Lett.* **B314** 132–138
- [11] Nadolsky P M and Yuan C P 2003 *Nucl. Phys.* **B666** 31–55
- [12] de Florian D and Vogelsang W 2010 *hep-ph/1003.4533*
- [13] Kotwal A V and Stark J 2008 *Ann. Rev. Nucl. Part. Sci.* **58** 147–175
- [14] Nakagawa I *et al.* 2007 *AIP Conf. Proc.* **915** 912–915
- [15] Makdisi Y I *et al.* 2007 *AIP Conf. Proc.* **915** 975–978
- [16] Grebenyuk O *et al.* 2009 *RHIC-AGS Users' Meeting*
- [17] Bridgeman A *et al.* 2010 *APS Spring Meeting 2010*
- [18] Corliss R *et al.* 2010 *APS Spring Meeting 2010*
- [19] Sjostrand T *et al.* 2001 *Comput. Phys. Commun.* **135** 238–259
- [20] de Florian D *et al.* 2005 *Phys. Rev.* **D71** 094018